Liquid Crystals
Publication details, including instructions for authors and subscription information:
http://www.informaworld.com/smpp/title~content=t713926090

A ^{2}H NMR study of order and dynamics in the cubic I_1 phase of the dodecyltrimethylammonium chloride/water system

Maria Törnblom[a]; Ruslan Sitnikov[a]; Ulf Henriksson[a]
[a] Division of Physical Chemistry, Royal Institute of Technology, S-100 44 Stockholm, Sweden,

Online publication date: 06 August 2010

To cite this Article Törnblom, Maria , Sitnikov, Ruslan and Henriksson, Ulf(2000) 'A ^{2}H NMR study of order and dynamics in the cubic I_1 phase of the dodecyltrimethylammonium chloride/water system', Liquid Crystals, 27: 7, 943 — 955
To link to this Article: DOI: 10.1080/02678290050043905
URL: http://dx.doi.org/10.1080/02678290050043905

LIQUID CRYSTALS, 2000, VOL. 27, NO. 7, 943–955

A ^{2}H NMR study of order and dynamics in the cubic I_1 phase of the dodecyltrimethylammonium chloride/water system

MARIA TÖRNBLOM, RUSLAN SITNIKOV and ULF HENRIKSSON*

Division of Physical Chemistry, Royal Institute of Technology, S-100 44 Stockholm, Sweden

(*Received 6 December 1999; accepted 9 February 2000*)

The micellar cubic phase I_1 of the dodecyltrimethylammonium chloride (C_{12}TACl)/water system has been studied by ^{2}H NMR spectroscopy. Relaxation rates of selectively deuteriated surfactant were measured at several frequencies down to 0.5 MHz in the temperature range 25–61°C. The results are interpreted within models for the reorientational dynamics in I_1 phases and it is concluded that the remaining order after surface diffusion and aggregate rotation is small and does not vary substantially with temperature. The results are discussed in relation to the two prevailing models for the structure of these phases as suggested (separately) by Fontell and Vargas. At 0°C the ^{2}H NMR spectrum from perdeuteriated *n*-dodecane solubilized in this phase shows static quadrupole splittings with a magnitude that is in good agreement with the results obtained from the analysis of the relaxation data.

1. Introduction

In most amphiphile/water systems the micelles are predominantly spherical or nearly spherical (globular) only at low concentrations. As the concentration rises, rod-like aggregates start to predominate and when the concentration is high enough for the gain in the free energy of aggregate interaction to overcome the entropy loss associated with the ordering, hexagonal phases are formed. In a few systems, however, the conditions for the formation of rod-like aggregates are not met before this solubility limit is reached. In these the hexagonal phase is preceded by a liquid crystalline phase with cubic symmetry, usually denoted I_1 [1–3]. The C_{12}TACl system [4] (figure 1) is one of the very few two-component ionic surfactant/water systems [4–6] where an I_1 phase is formed. These are otherwise more common in phospholipid [7, 8] or non-ionic surfactant systems [9–13] and in three-component surfactant/water/hydrocarbon systems [14, 15]. Most I_1 phases discovered up to 1990 are listed in [1].

I_1 phases have very high viscosities and interesting acoustic properties; they were early recognized as separate from the micellar solution phase [4]. Due to the cubic symmetry they are optically isotropic and it was not until X-ray methods were applied that their highly ordered structure was discovered [16, 17]. It was also these studies that first assigned I_1 phases to the space group $Pm3n$ (less likely $P43n$). It was later shown by NMR self-diffusion measurements [18] that the non-polar pseudo-phase in the I_1 phase in the C_{12}TACl/water system is discontinuous, i.e. the structure is formed by closed aggregates, as opposed to the V_1 phases occurring

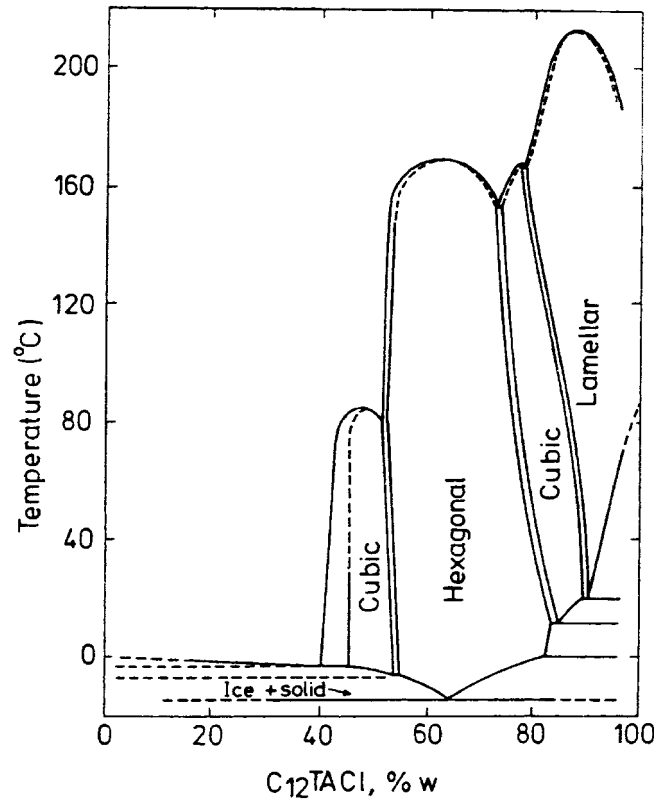

Figure 1. Phase diagram for the C_{12}TACl/water system. After Balmbra *et al.* [16].

* Author for correspondence; e-mail: ulf@physchem.kth.se

at concentrations between the hexagonal and the lamellar phase where both pseudo-phases are continuous. In the binary non-ionic system $C_{12}EO_{12}$/water three different I_1 phases have recently been found and assigned to the space groups *Pm*3*n*, *Im*3*m* and *Fm*3*m* by X-ray diffraction [13].

The majority of I_1 phases studied have been assigned to the space group *Pm*3*n* [1] and two models have emerged for the structure of this phase. These are similar in their basic overall structure, with eight aggregates in the unit cell, six of which are restricted in their rotation and arranged two and two perpendicular to or along what we will later refer to as the 'cubic' directors on the faces of the unit cube, in a fashion shown by figure 2. (Each of the aggregates depicted in the figure contributes 1/2 to the unit cell.) There are also spherical or isotropically reorienting aggregates centred in the corners and in the centre of the unit cube, together contributing a further two aggregates to the unit cell. The difference between the two models lies in the shape and the rotational order of the aggregates. The basic structure was first proposed by Fontell *et al.* [19] and is based on the crystal structure of some diatomic molecules. In this model all aggregates are prolate in form and the restricted aggregates are arranged with their symmetry axes at right angles to the cubic directors and free to rotate in planes perpendicular to these, see figure 2. Vargas *et al.* [20] later suggested that the two disordered aggregates are spherical and the six restricted ones are oblate with their symmetry axes coinciding with the cubic directors.

Much of the experimental evidence that has been collected since the ordered structure of I_1 phases was discovered support the main features of these structural models. Aggregation number measurements by fluorescence quenching [21–23] have shown that the aggregates are not spherical in the systems under consideration and this has been confirmed by field-dependent relaxation measurements [24, 25]. ^{14}N, ^{2}H and ^{31}P NMR spectra from I_1 phases in two systems of large amphphiles [22, 26], where the final averaging of interactions was incomplete, show a superposition of one anisotropic and one isotropic signal and support the notion that there are two types of aggregates with different rotational order, at least in the I_1 phases of these systems.

It has earlier only been through NMR spectra with quadrupole splittings or chemical shift anisotropies that it has been possible to quantify the remaining order at the aggregate sites, i.e. the composite aggregate-rotation order parameter, S_{DM} [27] (see below). The symmetry of I_1 phases allows for full motional averaging of any angular dependent interaction; for simple surfactants all the motional processes carrying out this averaging are fast enough to yield isotropic NMR signals without any structure information. In these cases, structure information can still be extracted through the contributions from different motional processes to the relaxation rates R_1 and R_2 at different magnetic field strengths or, explicitly, Larmor frequencies ω. For these experiments ^{2}H is the best suited nucleus since the Larmor frequencies fall in the same frequency range as the most interesting part of the relaxation dispersion and the relaxation rates follow simple equations. ^{2}H can also readily be selectively introduced into the hydrocarbon tail of the surfactant, in the α-position to the head group. For a quadrupole nucleus the entire accessible information content,

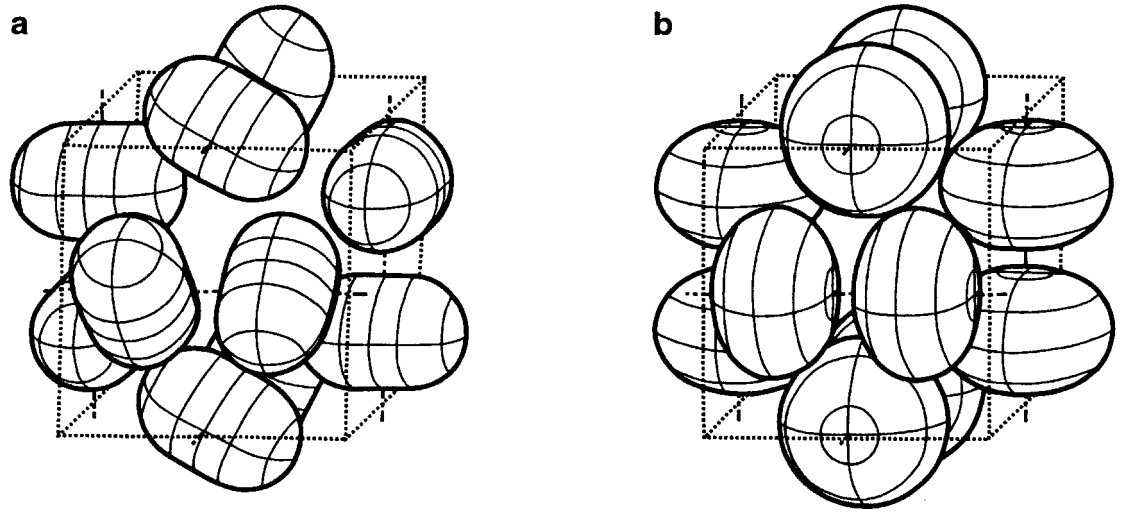

Figure 2. The arrangement and shape of the restrictedly rotating aggregates in the models for the I_1 phase according to: (*a*) Fontell *et al.* [19] and (*b*) Vargas *et al.* [20]. The dash-dotted lines through the centres of the aggregates signify cubic directors discussed in the text. The spherical or isotropically reorienting aggregates in the centre and corners of the unit cube have been left out for visibility.

including the behaviour at zero field, is contained in the dispersion of the longitudinal relaxation rate R_1, combined with the transverse relaxation rate R_2 at a single field.

In this work we present a ^2H NMR study of the I_1 phase of the $C_{12}TACl$/water system at 50 wt% surfactant which has been assigned to the space group $Pm3n$ [16, 17, 19, 20]. In this I_1 phase the signal from the α-deuteriated surfactant does not deviate significantly from Lorentzian shape even at 0°C. Perdeuteriated *n*-dodecane was therefore solubilized in the I_1 phase to function as an 'order probe'. At 0°C the dodecane yielded an NMR spectrum from which the quadrupole splittings could be estimated. At four higher temperatures the field-dependence of the relaxation rates for the α-deuteriated surfactant was measured and apart from the order, the dynamics of the different motional processes of the surfactant molecules could also be studied. This particular system has been studied previously with field-dependent relaxation [24] and the measurements were evaluated within the empirical three-step model, but now we have at our disposal two important new tools. The first is spectrometer equipment making NMR measurements possible in the previously inaccessible frequency range between 0.5 and 2.0 MHz [28]. The other is a framework for the derivation of theoretical relaxation rates in systems of cubic symmetry [29, 30] enabling the interpretation of experimental results in physical quantities such as order parameters and rates of dynamic processes. We have also performed the measurements over a wider temperature range than in the earlier study to take full advantage of the possibilities offered by these extensions.

2. Dynamic models and relaxation theory

In order to find a model connecting structure to relaxation rates, we follow the averaging of the quadrupolar interaction due to fluctuations in the orientation of the molecule-fixed principal axis of the electric field gradient tensor at the ^2H nucleus, z_P, relative to the laboratory-fixed frame which is defined by the direction of the applied magnetic field, z_L. As no experimental evidence suggests the contrary, we assume that the processes of molecular and aggregate dynamics are essentially the same as for micelles in isotropic solutions [31–33]. The averaging is treated as a stepwise process in a hierarchy of frames, each defined by a director, z_j [32]. With the frames chosen properly, a single motional mechanism mediates the fluctuations of the orientation of z_j relative to the nearest higher frame in the hierarchy, z_i. In each of these steps there is partial averaging of the interactions characterized by a second rank order parameter

$$S_{ij} = \langle D^2_{00}(\Omega_{ij})\rangle = \frac{1}{2}\langle 3\cos^2\theta_{ij} - 1\rangle \qquad (1)$$

where $D^2_{00}(\Omega_{ij})$ is a second rank Wigner matrix element [34]. This order parameter corresponds to the fraction of the initial interaction not averaged out by the motion.

The first motional step is the local motions of the surfactant molecule relative to the surface normal z_M, at the site of its head group on the aggregate surface. This is actually a complex process, involving a number of mechanisms, but as it occurs on a time scale at least two orders of magnitude faster than the motional processes responsible for the observed dispersion of the relaxation rates in the accessible field range [24, 25] we do not propose a physical model, but let it be represented by the two basic parameters of the two-step model [31]: the 'local' order parameter S_{MP}, which is a measure of the confinement of the molecule, and the effective 'fast' correlation time τ^{MP}.

In the second step the averaging of the orientation of the surface normal relative to the aggregate symmetry axis z_A is caused by the lateral diffusion of the molecules over the aggregate surface. Halle [32] has treated this as free surface diffusion with a constant diffusion coefficient and presented numerical methods, as well as simple analytic approximations for the calculation of the corresponding time correlation functions. The corresponding order parameter S_{AM} is given by equation (1) with the average taken over the aggregate surface and it varies substantially with shape for aggregates of equal aggregation number.

In micellar solutions of low to moderate concentrations, the final randomization of orientations proceeds by the free Brownian rotational diffusion of the aggregates [32, 35, 36]. In I_1 phases this is not the case for all the aggregates. One of the basic features common to both structural models discussed here is that the aggregates situated on the unit cube faces are restricted from rotating through all angles of space with equal probability through interaction with their neighbours. There is hence non-vanishing rotational order in both models, but due to the differences in the arrangement of the aggregates the rotational order parameters differ in sign as well as in magnitude for the two models. In the Vargas structural model in its most extreme form, the aggregate symmetry axes z_A are perfectly aligned along the cubic directors z_D (see figure 2), and the aggregates are only allowed to perform spinning motion around these. This is called full rotational order and $S_{DA} = 1$. In Fontell's model, again in the limit of highest possible order, the z_As are confined to planes perpendicular to the z_D, but free to rotate in these planes giving $S_{DA} = -1/2$. We will in the further treatment assume that this rotation has a time evolution that is faster than that of molecular or aggregate exchange processes, despite the fact that geometric calculations show that it has to be concerted and thereby strongly collective. In a real phase structure it may well

be that the confinement of the aggregate directors is not as strict as in the corresponding idealized models and the magnitude of S_{DA} is lower. For the molecules in the restricted rotation aggregates, the quadrupolar interaction is thus not averaged out completely by the rotational motion. The remaining interaction strength corresponds, for a spin = 1 nucleus, to a splitting

$$\Delta\nu = \frac{3}{4}\chi|S_{DM}S_{MP}| \tag{2}$$

in the Pake doublet from a powder sample. In this equation we have also defined the composite rotation-aggregate order parameter $S_{DM} = S_{DA}S_{AM}$. The orientation of the two remaining aggregates in the unit cell is, in both structural models, completely randomized already by the rotation.

For the NMR signals from I_1 phases to be isotropic there must be at least one additional motional process, the so called the 'cubic motion', that completely averages out the last remnant of the interaction. This is probably an exchange process that distributes molecules or aggregates between different sites in the unit cell with different z_D. NMR self-diffusion data from three component systems [23] tell us that molecular exchange between aggregates is faster than the exchange of aggregates between different sites and at least should contribute the main part of the rate of this averaging.

The relaxation behaviour of the ^2H nucleus is determined by the second rank spherical time correlation functions (TCFs) in the laboratory-fixed frame through their Fourier–Laplace cosine transforms, the spectral densities. These TCFs describe the average time evolution of the fluctuations of the the laboratory frame components, F_k^L, of the normalized second rank spherical electric field gradient tensor due to the stochastic reorientation of the spin-bearing molecules. The spherical TCFs for the entire averaging process in the laboratory frame are by definition:

$$G_k^L(\tau;\theta_{LC},\varphi_C) = \langle F_k^{L*}[\Omega_{LP}(0)]F_k^L[\Omega_{LP}(\tau)]\rangle . \tag{3}$$

In a system of cubic symmetry, as in other ordered systems, the $G_k^L(\tau;\theta_{LC},\varphi_C)$ for the different components, $k = 0, 1, 2$, are different and they also depend on the orientation of the unit cell or crystal frame, with z-axis z_C, relative to z_L which is given by the angles θ_{LC} and φ_C

In theory this means that the different spectral densities can be extracted in a model-free way by measuring the orientation dependence of the relaxation rates, if an oriented sample can be prepared [29]. Samples of cubic phases prepared by simple mixing, like the one used in this study, are however polycrystalline. If the diffusion of molecules over crystallites with different orientations is fast enough compared with the difference in relaxation rates, the measurable correlation function is the spherical average of G_k^L [29]

$$G_{iso}^L(\tau) = \frac{1}{4\pi}\int_0^{2\pi} d\varphi_C \int_0^{\pi} d\theta_{LC} \sin\theta_{LC} G_k^L(\tau;\theta_{LC},\varphi_C). \tag{4}$$

This function is independent of the index k, as for truly isotropic systems. In consequence there is only one laboratory frame spectral density

$$J_{iso}^L(\omega) = \int_0^{\infty} d\tau \cos\omega\tau\, G_{iso}^L(\tau) \tag{5}$$

and the equations for the quadrupolar relaxation rates in an isotropic system at Larmor frequency ω apply [37]

$$R_1(\omega) = T_1^{-1}(\omega) = \frac{3\pi^2}{4}\chi^2[2J_{iso}^L(\omega) + 8J_{iso}^L(2\omega)] \tag{6}$$

$$R_2(\omega) = T_2^{-1}(\omega) = \frac{3\pi^2}{4}\chi^2[3J_{iso}^L(0) + 5J_{iso}^L(\omega) + 2J_{iso}^L(2\omega)]. \tag{7}$$

In $G_{iso}^L(\tau)$ and $J_{iso}^L(\omega)$, the contribution from the 'fast' molecular motions can be separated from the 'slower' contributions in the framework of the two-step model [31] as in isotropic systems [30], and can be represented by the two parameters of this model (see above). The slow step consists, in our case, of the composite TCF for the averaging of the orientation of the molecular director (or surface normal) z_M relative to the crystal axis z_C, averaged over the powder and expressed in the laboratory frame; $G_{iso}^{L,CM}(\tau)$. The form of this function expressed in the crystal frame spherical TCFs has been derived by Halle [29]:

$$G_{iso}^{L,CM}(\tau) = \frac{1}{5}\sum_{l=0}^{2}(2-\delta_{l0})G_{l0}^{CM}(\tau). \tag{8}$$

In his paper, Halle also explicitly derived $G_{iso}^{L,CM}(\tau)$ for Fontell's I_1 structure within the motional model discussed earlier. In this derivation the assumption of time scale separation between the rotational and the cubic motion has been invoked for simplicity. (The formal derivation of the exact expression requires the application of the methods outlined in Appendix C of [30] or the calculation of a very large number of spherical TCFs.) In the treatment of the cubic motion, however, cubic directors were defined for the two isotropically rotating aggregates and these were allowed to contribute to the cubic order parameter. However, such directors cannot be defined since these aggregates are already spherically disordered by the rotational motion. The cubic order parameter for the entire unit cell is consequently not a well defined quantity. The procedure therefore results in an error in

the numerical factor for the cubic contribution to the total TCF, equation 7.19 in Halle's paper. A correct derivation accounts for the variation in S_{DA} and S_{AM} as well as the orientation of the cubic director over the eight sites in the unit cell. If the mechanism for the cubic motion is an exchange process, this gives for a general case of a cubic phase with the same basic structure as the Fontell and Vargas models:

$$G_{iso}^{L,CD} = \frac{1}{5}\langle S_{DA}^2 S_{AM}^2 \rangle \exp(-\tau/\tau^{CD}) \tag{9}$$

This expression has the character of an average over one contribution from the six restricted micelles, derived as in [29], and one from the two isotropically disordered micelles which is zero. A formally correct derivation must, however, account for the contribution of the disordered aggregates to the rate of the cubic motion. If the mechanism is molecular exchange and if re-entry into the original aggregate is allowed, the cubic motion correlation time τ^{CD} can be identified with

$$\tau^{CD} = \tau_{ex} \tag{10}$$

the mean residence time of the surfactant molecule in an aggregate [38].

With equation (9) and with the expression for the director frame rotation–diffusion TCFs (equation 7.10 in [29]) averaged over the eight aggregates, the general expression for $G_{iso}^{L,CM}(\tau)$ in any structure with the actual basic arrangement, but with aggregates of arbitrary rotational order and shape, is

$$\begin{aligned} G_{iso}^{L,CM}(\tau) = \frac{1}{5}\Bigg\{ & P_R\Bigg[S_{DA}^2 S_{AM(R)}^2 \exp(-\tau/\tau^{CD}) + S_{DA}^2 g_0^{AM(R)}(\tau) \\ & + S_{AM(R)}^2 \sum_{m=0}^{2} (2-\delta_{m0}) g_{m0}^{DA}(\tau) \\ & + \sum_{m=0}^{2}\sum_{n=0}^{2} (2-\delta_{m0})(2-\delta_{n0}) g_{mn}^{DA}(\tau) g_n^{AM(R)}(\tau) \Bigg] \\ & + P_I\Bigg[S_{AM(I)}^2 g_0^{LA}(\tau) + \sum_{n=0}^{2} (2-\delta_{n0}) g_n^{LA}(\tau) g_n^{AM(I)}(\tau) \Bigg] \Bigg\} \end{aligned} \tag{11}$$

with R denoting the restrictedly and I the isotropically reorienting micelles. $g_{mn}^{DA}(\tau)$, $g_n^{LA}(\tau)$ and $g_n^{AM(I)}(\tau)$ are the correlation functions of restricted rotation, isotropic rotation and surface diffusion, respectively and P_I is the fraction of molecules in the I-type of aggregates.

Upon transformation, equation (11) gives the contribution of the 'slow' aggregate related motions to the spectral density function, equation (5). To obtain the total spectral density according to the two-step model, the slow term is multiplied by S_{MP}^2 and the fast contribution added. The first term in this expression is a Lorentzian with correlation time τ^{CD} scaled by the factor

$$P_R S_{DA}^2 S_{AM}^2 S_{MP}^2 = P_R S_{DM}^2 S_{MP}^2. \tag{12}$$

A comparison with equation (2) shows that if this factor can be extracted from the relaxation rates, approximately the same information as is given by the splitting can be obtained.

For the two structural models discussed here, equation (11) simplifies somewhat. For the idealized Fontell model, i.e. with $S_{DA} = -1/2$, the S_{AM} equal for all aggregates, $P_R = 6/8$ and the correlation functions for strict in-plane rotation inserted into equation (11), we obtain

$$\begin{aligned} G_{iso}^{L,CM}(\tau) = & \frac{1}{5}\Bigg\{ S_{AM}^2 \Bigg[\frac{6}{8}\Bigg(\frac{1}{4}\exp(-\tau/\tau^{CD}) + \frac{3}{4}\exp(-\tau/\tau_{20}^{DA}) \Bigg) \\ & + \frac{2}{8}\exp(-\tau/\tau_{00}^{LA}) \Bigg] + \frac{6}{8}\sum_{m=0}^{2}\sum_{n=0}^{2} (2-\delta_{m0})(2-\delta_{n0}) \\ & \times [d_{mn}^2(\pi/2)]^2 \exp(-\tau/\tau_{mn}^{DA}) g_n^{AM}(\tau) \\ & + \frac{2}{8}\sum_{n=0}^{2} (2-\delta_{n0}) \exp(-\tau/\tau_n^{LA}) g_n^{AM}(\tau) \Bigg\} \end{aligned} \tag{13}$$

with the correlation times for in-plane rotation

$$\frac{1}{\tau_{mn}^{DA}} = m^2 R_\perp + n^2 R_\parallel \tag{14}$$

and those for the isotropically reorienting aggregates [36]

$$\frac{1}{\tau_n^{LA}} = (6-n^2) R_\perp + n^2 R_\parallel \tag{15}$$

where $R_\parallel$ and $R_\perp$ are the rotational diffusion coefficients parallel and perpendicular to the aggregate symmetry axis. In the implementation of these equations, we have assumed that the spinning mode of the rotation is undisturbed by the tightly packed structure and that $R_\parallel$ is therefore determined by hydrodynamic forces [35, 39, 40] as in dilute solution. As for the tumbling, geometric calculations show that if all aggregates are non-spherical it cannot take place independently, but has to be concerted even for the isotropically reorienting aggregates. It is thus not Brownian, but a collective process and we have refrained from proposing a physical model for $R_\perp$; instead we have treated it as a free parameter varied in the fittings of the theoretical models to experimental data.

With the assumption that the rate of the tumbling is small compared with that of the spinning, which is

implemented by Halle [29], these equations reduce to

$$G_{\mathrm{iso}}^{\mathrm{L,CM}}(\tau)=\frac{1}{5}\left\{S_{\mathrm{AM}}^2\left[\frac{6}{8}\left(\frac{1}{4}\exp(-\tau/\tau^{\mathrm{CD}})+\frac{3}{4}\exp(-4R_\perp\tau)\right)+\frac{2}{8}\exp(-6R_\perp\tau)\right]+\sum_{n=0}^{2}(2-\delta_{n0})\exp(-n^2R_\parallel\tau)g_n^{\mathrm{AM}}(\tau)\right\} \quad (16)$$

which is the correct form of equation 7.24 in Halle's paper. In the zero time limit this expression goes to

$$G_{\mathrm{iso}}^{\mathrm{L,CM}}(0)=\frac{1}{5} \quad (17)$$

as do the TCFs in equations (11) and (13), which is required for an isotropically averaged correlation function. This follows from equation (8) in combination with the orthogonality of the Wigner functions [34].

In our earlier work on micelles [33], we utilized the single exponential initial slope approximation [32] for the correlation functions for the diffusion over the spherocylindrical aggregate surfaces, $g_n^{\mathrm{AM}}(\tau)$ and it may be used here as well, especially since the axial ratios of the aggregates are small. (Explicit expressions for the diffusion correlation times, τ_n^{AM}, of spherocylinders in terms of the lateral diffusion coefficient, D_{lat}, and varying aggregate dimensions have been given in the appendix of [33].) With this approximation and with the two-step model [31] applied to the fastest motions, the total laboratory frame isotropic spectral density for the idealized Fontell structure, obtained by the transformation of equation (13), is a sum of Lorentzian terms

$$J_{\mathrm{iso}}^{\mathrm{L}}(\omega)=\frac{1}{5}\left\{S_{\mathrm{MP}}^2\left[S_{\mathrm{AM}}^2\left(\frac{3}{16}\frac{\tau^{\mathrm{CD}}}{1+(\omega\tau^{\mathrm{CD}})^2}+\frac{9}{16}\frac{\tau_{20}^{\mathrm{DA}}}{1+(\omega\tau_{20}^{\mathrm{DA}})^2}+\frac{1}{4}\frac{\tau_0^{\mathrm{LA}}}{1+(\omega\tau_0^{\mathrm{LA}})^2}\right)+\frac{3}{4}\sum_{m=0}^{2}\sum_{n=0}^{2}(2-\delta_{m0})(2-\delta_{n0})[d_{mn}^2(\pi/2)]^2\times g_n^{\mathrm{AM}}(0)\frac{\tau_{mn}^{\mathrm{DM}}}{1+(\omega\tau_{mn}^{\mathrm{DM}})^2}+\frac{1}{4}\sum_{n=0}^{2}(2-\delta_{n0})g_n^{\mathrm{AM}}(0)\times\frac{\tau_n^{\mathrm{LM}}}{1+(\omega\tau_n^{\mathrm{LM}})^2}\right]+(1-S_{\mathrm{MP}}^2)\tau^{\mathrm{MP}}\right\} \quad (18)$$

with the composite correlation times given by

$$\frac{1}{\tau_{mn}^{\mathrm{DM}}}=\frac{1}{\tau_{mn}^{\mathrm{DA}}}+\frac{1}{\tau_n^{\mathrm{AM}}} \quad (19)$$

$$\frac{1}{\tau_n^{\mathrm{LM}}}=\frac{1}{\tau_n^{\mathrm{LA}}}+\frac{1}{\tau_n^{\mathrm{AM}}}. \quad (20)$$

For the Vargas structural model with $S_{\mathrm{DA}}=1$ and $S_{\mathrm{AM(I)}}=0$, the TCF has the simple form

$$G_{\mathrm{iso}}^{\mathrm{L,CM}}(\tau)=\frac{1}{5}\left\{P_{\mathrm{R}}\left[S_{\mathrm{AM}}^2\exp(-\tau/\tau^{\mathrm{CD}})+\sum_{n=0}^{2}(2-\delta_{n0})\exp(-\tau/\tau_{nn}^{\mathrm{DA}})g_n^{\mathrm{AM(R)}}(\tau)\right]+P_{\mathrm{I}}\exp(-\tau/\tau^{\mathrm{LA(I)}})\exp(-\tau/\tau^{\mathrm{AM(I)}})\right\} \quad (21)$$

with index I denoting the spherical aggregates. The rotational correlation times for the spinning motion are [32]

$$\frac{1}{\tau_{nn}^{\mathrm{DA}}}=n^2R_\parallel. \quad (22)$$

An exponential approximation for the diffusion correlation functions can be applied to oblate aggregates as well as prolate. If this is done, the spectral density obtained by the transformation of equation (21) will be a sum of Lorentzians in parallel to equation (18).

3. Experimental

Dodecyltrimethylammonium chloride (C_{12}TACl), selectively deuteriated in the α-position to the head group, was synthesized as described in an earlier paper [24]. A sample was prepared with purified water at a surfactant concentration of 50 wt %. Non-deuteriated surfactant (Fluka) and perdeuteriated *n*-dodecane (Larodan) were used as received. A 50% sample of this surfactant was prepared and *n*-dodecane-d_{26} added corresponding to a molar ratio of 1 : 78. Another sample with the same additive : surfactant ratio, but with a concentration in the hexagonal regime (65 wt % surfactant) was also prepared.

^{2}H NMR measurements were performed with a Bruker MSL 200/90 equipped with a variable-field iron core magnet rebuilt to work down to 0.5 MHz [28] (at 0.5–13.8 MHz), the MSL or a DMX 200 equipped with a 4.7 T cryomagnet (at 30.7 MHz), a Bruker AMX 300 (at 46.1 MHz), a Bruker AM 400 (at 61.4 MHz) and a Bruker DMX 500 (at 76.8 MHz). The surfactant macroscopic self-diffusion coefficients were measured in the same sample with a stimulated echo PGSE-sequence on the AMX 300 equipped with a gradient aggregate manufactured by Digital Specialities and a 10 mm 300 MHz ^{1}H gradient probe from Cryomagnet Systems.

Relaxation rates and self-diffusion coefficients were measured at 25.1, 41.0, 55.2 and 60.6°C. The temperature was monitored by a Bruker VT 100 unit (at 0.5–30.7 MHz and 41, 55 and 61°C) or by B-VT 2000 or B-VT 3000 units. It was always controlled before and, sometimes, between measurements with an external

thermometer with a PT 100 sensor mounted in an NMR tube. We estimate the total standard variations in temperature between measuring points to be ± 0.4°C at 25°C, ± 0.5°C at 41 and 55°C and ± 0.6°C at 61°C.

At each temperature ^2H R_1s were measured at 14–17 frequencies between 0.5 and 76.8 MHz with the standard inversion recovery method, while R_2 was determined at 30.7 MHz with the CPMG method. The 2.0 MHz R_1 and the R_2 measurements were repeated several times to estimate the uncertainties in the measurements. With a sample of this concentration, the S/N ratios in the spectra are very good even at low frequencies and the standard deviations in the T_1 and T_2 determinations are ± 1% or lower at 2.0 MHz and upwards. At the lowest frequencies, however, the signal is weak despite the high concentration, giving uncertainties in T_1 of around ± 3% at 1.0 MHz and ± 4–9%, depending on experiment time, at 0.5 MHz. To these uncertainties should be added contributions from the temperature variation discussed above which we have estimated with Arrhenius interpolation to be ± 1–2% in T_1 at low frequencies, ± 0.5–1% at the higher frequencies, and ± 2–3% in the R_2 point. These estimated errors correspond well with the RMS-deviations of the fittings as can be seen in the figures of the next section.

4. Results

In the actual system, the signal from the α-deuteriated surfactant was isotropic down to the lower temperature limit of the one-phase region. A sample with non-deuteriated surfactant was therefore prepared with per-deuteriated *n*-dodecane ($C_{12}D_{26}$) added as a probe to an amount corresponding to approximately one molecule per aggregate. This was done in the hope that a large hydrophobic additive would have a long enough residence time [23] to yield non-averaged spectra. This sample was, on visual inspection, as stiff as the one containing the surfactant only and optically isotropic at all measurement temperatures; it seems that the addition of the alkane did not cause a phase transition. At 25°C and above, the spectrum from the dodecane was isotropic but at 0°C the line was bottle-shaped, as can be seen in figure 3 (*a*). The line shape bears a reasonable resemblance to the ^2H and ^{14}N lines in [26], though it is much narrower. The spectrum consists of a superposition of Pake doublets from the six non-equivalent segments of the dodecane residing in the restrictedly rotating aggregates, the unsplit signal from dodecane in the isotropically reorienting aggregates and also the signals from naturally occurring deutrons in the surfactant chains. (The small signals on the high frequency side originate in naturally occurring deutrons in the surfactant and in water.) With resolution enhancement by sine-bell multiplication, as in figure 3 (*b*), the largest quadrupole splitting can be

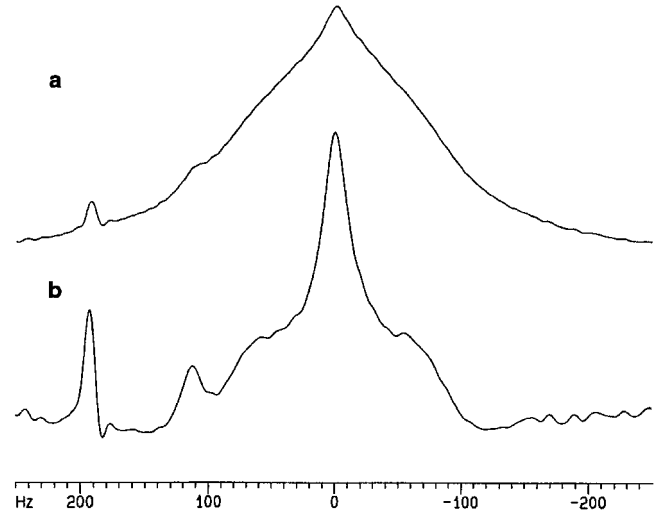

Figure 3. The ^2H NMR spectrum at 46.1 MHz and 0°C of perdeuteriated *n*-dodecane solubilized in the I_1 phase of the $C_{12}ACl$/water system. (*a*) As recorded; (*b*) with resolution enhancement through sine-bell multiplication.

determined to be 149 ± 5 Hz. This splitting corresponds to the one given by equation (2). The corresponding splitting in the spectrum of $C_{12}D_{26}$, solubilized in the hexagonal phase at the same temperature, is 1174 ± 20 Hz. With the assumption that the local order parameter S_{MP} is independent of aggregate shape, we get $|S_{DM}| = 0.063 \pm 0.004$ in the I_1 phase at 0°C. It should also be pointed out that the occurrence of anisotropic lines in the spectrum of an additive while the signal from the surfactant is fully averaged, is evidence that molecular exchange is the dominating mechanism for the final averaging of the quadrupole interaction (the cubic motion) for the surfactant.

To obtain order information at higher temperatures, the relaxation dispersion over a large frequency range had to be measured and analysed. For these measurements it is advantageous to use the deuteriated surfactant because of the relatively high local order parameter. The results of these measurements are shown in figures 4 and 5. The dispersions of these relaxation rates all have a three-step character, even if the slowest step at the two lowest temperatures lies outside the available frequency range and is only visible in the level of the R_2 points. We showed in the theory section that the first term in the spectral density function is a Lorentzian with the correlation time τ^{CD} scaled by the factor $P_R S_{DM}^2 S_{MP}^2$. The three-step character of the data sets means that the rotation and diffusion terms of the spectral density (corresponding to all terms of equation (9) except the first one) are not distinguishable, i.e. their sum makes up one effective step in the observed spectral density. If this step has an approximately Lorentzian shape, a model-independent evaluation of the experimental

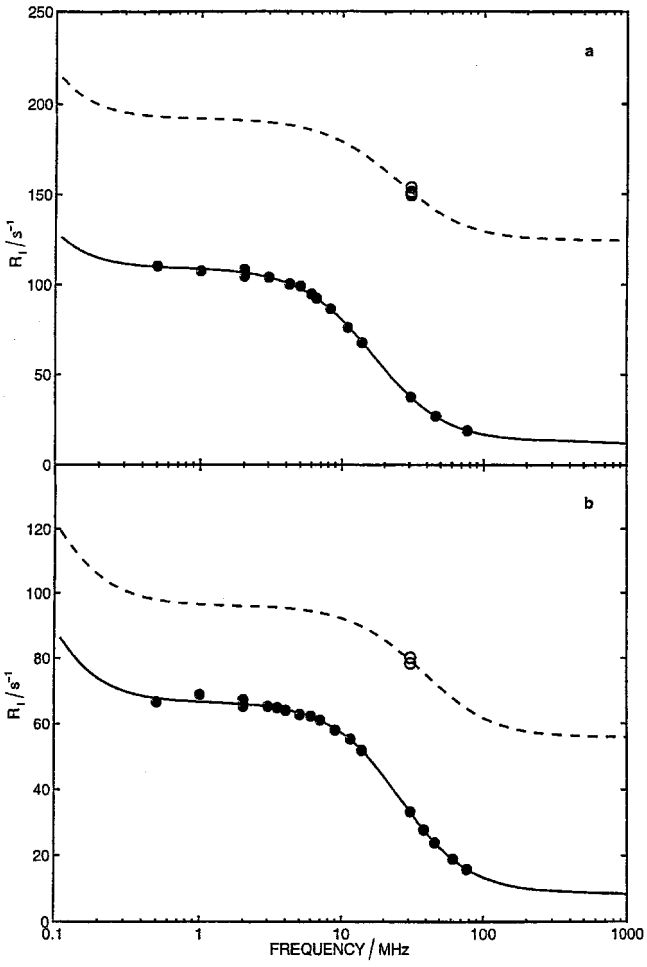

Figure 4. ^{2}H R_1 (filled symbols) and R_2 (open symbols) for α-deuteriated C_{12}ACl in the I_1 phase. (*a*) At 25°C; (*b*) at 41°C. The solid and dashed lines represent fittings of theoretical relaxation rates for Fontell's model [19] with spherocylindrical aggregates as described in the text. The fitting results are given in table 3.

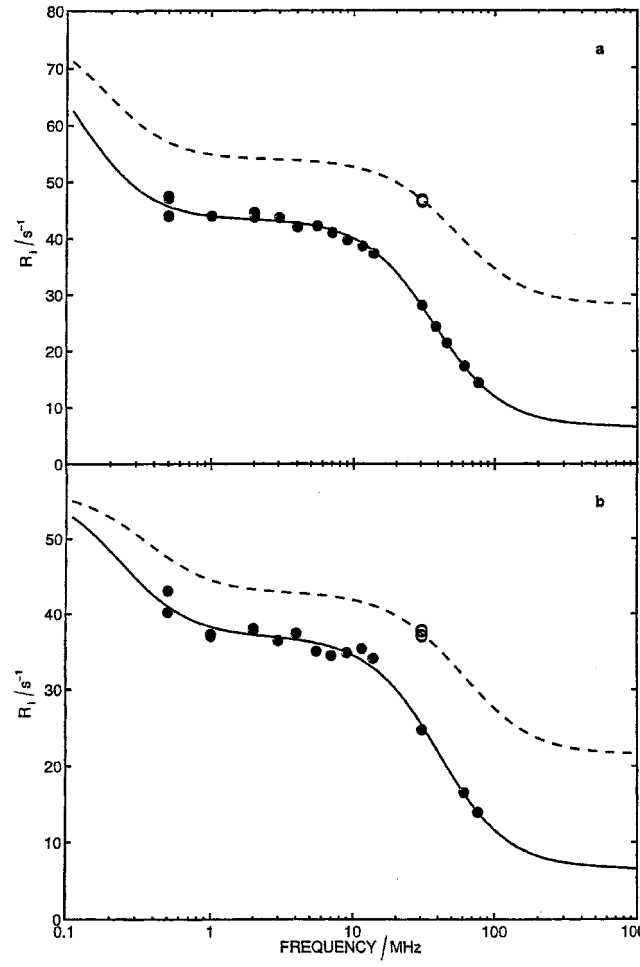

Figure 5. ^{2}H R_1 (filled symbols) and R_2 (open symbols) for α-deuteriated C_{12}ACl in the I_1 phase. (*a*) At 55°C; (*b*) at 61°C. The solid and dashed lines represent fittings of theoretical relaxation rates for Fontell's model [19] with spherocylindrical aggregates as described in the text. The fitting results are given in table 3.

relaxation rates can be made by fittings of equations (6) and (7) with the spectral density, J^{L}_{iso}, given by the Lorentzian three-step model [41]:

$$J^{L}(\omega) = \frac{1}{5}\left\{S^2_{MP}\left[s^2\frac{\tau^{vs}}{1+(\omega\tau^{vs})^2} + (1-s^2)\frac{\tau^{s}}{1+(\omega\tau^{s})^2}\right] + (1-S^2_{MP})\tau^{MP}\right\}. \quad (23)$$

Following the reasoning above we may now identify τ^{vs} with τ^{CD} and s with $\sqrt{P_R}|S_{DM}|$.

Fittings of equations (6), (7) and (23) were performed with a program based on the TWOSTEP [42] program but with an improved routine for the Monte Carlo error analysis. This program minimizes the relative RMS-deviation of the theoretical relaxation rates from the experimental. In these fittings, the quadrupole coupling constant χ was set to 170 kHz as suggested by Jansson *et al.* [43] The choice is based on the ratios of the ^{2}H to the ^{13}C relaxation rates for the $C_{12}TA^+$ monomer which were measured during the course of this work. This ratio varied between 9 and 11.5 at the different temperatures and this is closer to the values found for $C_{10}A^+$ in the above-cited work than to the ratios measured by Söderman for hexanoate ions [44].

The fitted s and τ^{vs} are given in table 1. The two parameters can be evaluated separately when at least part of the dispersion of the 'very slow' step extends into the frequency range studied which, as noted, is not the case at the two lowest temperatures. For these only the product $s^2\tau^{vs}$ can be obtained. (It is, in principle, this product that was determined in the earlier field-dependent relaxation investigation of the C_{12}TACl/water I_1 phase [24] though it was given in other units.) To

Table 1. Parameters obtained by fitting the Lorentzian three-step model, equation (23), to the relaxation data.

T/°C	s	τ^{vs}/μs	$s^2\tau^{vs}$/μs	RMS dev./%
25.1			$0.0164^{+0.0006}_{-0.0008}$	1.4
41.0			$0.0063^{+0.0006}_{-0.0005}$	1.5
55.2	$0.060^{+0.006}_{-0.008}$	$0.69^{+0.20}_{-0.13}$		2.0
60.6	$0.066^{+0.010}_{-0.010}$	$0.34^{+0.10}_{-0.08}$		2.3

obtain $|S_{DM}|$ the s-values of table 1 should be divided by ~ 0.90 to account for the factor $\sqrt{P_R}$. This gives $S_{DM} \sim 0.065$–0.075 which, within the uncertainties, is equal to the 0°C value obtained from the observed splittings for solubilized $C_{12}D_{26}$; it seems this order parameter does not vary much in the temperature interval studied.

These results can be be verified since an independent source of information on τ^{CD} is available through the measured self-diffusion coefficient of the surfactant molecules. If we assume that the cubic motion is an exchange process and if the self-diffusion of the surfactant is a random walk between neighbouring aggregates, the average residence time in each of these can be calculated from the self-diffusion coefficient and the average square jump length $\langle l^2 \rangle$ [23]:

$$\tau_{ex} = \frac{\langle l^2 \rangle}{6D}. \tag{24}$$

In practice this procedure gives an upper limit for the residence time, since we can expect the measured self-diffusion coefficient to be affected by lattice defects and grain boundaries. With the assumption made in the derivation of equation (10), i.e. that jumps can take place between any neighbouring aggregates, the relation between the squared average jump length and the cell parameter a is

$$\langle l^2 \rangle = 0.305a^2 \tag{25}$$

which is the actual mean square displacement, not the projection on any of the crystal axes.

The self diffusion coefficients at the four temperatures measured by PGSE are given in table 2, as are the calculated maximum residence times and the other input parameters required to calculate these. It is interesting to note that the results at 55 and 61°C are within the uncertainties equal to the τ^{vs} evaluated from the relaxation dispersion. This fact supports the dynamic model we have applied. If we assume that this is also the case at the two lower temperatures, $|S_{DM}| \sim 0.055$–0.075 is obtained from the products given in table 1 and this result does not deviate substantially from what was obtained by fitting of the three-step model to the relaxation data at the two higher temperatures.

Table 2. Self-diffusion coefficients for the surfactant in the I_1 phase.

T/°C	D/μm^2 s^{-1}	n_a[a]	a[b]/Å	τ_{ex}[c]/μs
25.1	0.580 ± 0.004	89	85.4[d]	6.39 ± 0.05
41.0	1.69 ± 0.01	82	83.1[e]	2.08 ± 0.02
55.2	5.00 ± 0.04	77	81.4[e]	0.673 ± 0.005
60.6	9.53 ± 0.19	75	80.7[e]	0.347 ± 0.007

[a] Aggregation numbers from the results of Fletcher [21] by interpolation.
[b] Unit cell parameter.
[c] Calculated from equations (24) and (25).
[d] From Fletcher [21].
[e] The 25°C result scaled by $\sqrt[3]{n_a}$.

To interpret the results obtained above we can compare them to theoretical S_{DM} values for different models. If all aggregates had been spherical, S_{DM} would have been zero and there would not have been a third step in the relaxation dispersion. We can therefore conclude that this is not the case at any of the temperatures studied. This result is in full accordance with the aggregation numbers found by Fletcher [21], see table 2 (the aggregation number of the largest possible spherical micelle is 56). Theoretical composite order parameters $S_{DM} = S_{DA}S_{AM}$ for four different structures with non-spherical aggregates are presented in figure 6; Fontell's model ($S_{DA} = -1/2$) with the aggregates shaped as cylinders with spherical end caps [33] (spherocylinders) or as prolate ellipsoids [32], and the Vargas model ($S_{DA} = 1$) with flat discs with semi-toroidal rims [45] or with oblate ellipsoids [32]. The diffusion or aggregate

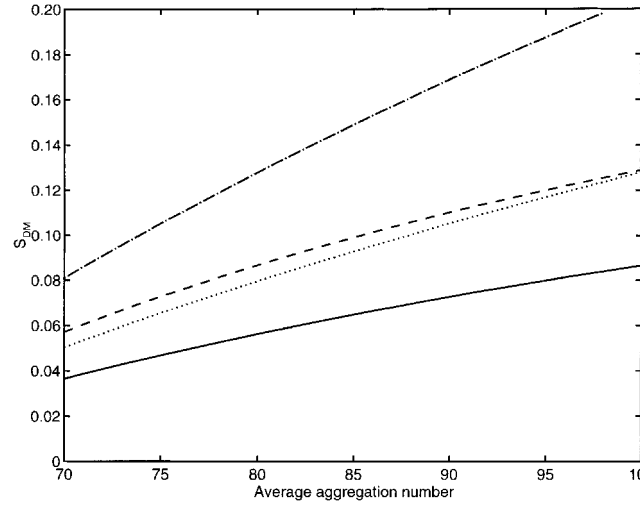

Figure 6. Theoretical composite aggregate-rotation order parameters S_{DM} for Fontell's structural model [19] ($S_{DA} = -1/2$) with aggregates shaped as spherocylinders (—) or prolate ellipsoids (- - -), and for the Vargas model [20] ($S_{DA} = 1$) with semi-toroidal discs (···) or oblate ellipsoids (–·–).

order parameter S_{AM} is a function of the axial ratio, ρ, of the aggregate which was determined from the aggregation numbers, setting the volume of a hydrocarbon chain to 350.2 Å^3 and the hydrocarbon core radius of the aggregates to the length of the chain in the all-*trans*-conformation, 16.7 Å [46]. S_{AM} is always negative for prolate shapes and always positive for oblate shapes.

Figure 6 shows that there are large differences in S_{DM} between the different cases at higher aggregation numbers (low temperature). The differences between the two models is not surprising. It is perhaps more surprising that differences in aggregate shape within the same structural model has as big an influence. This reflects both the larger axial ratios of spheroidal, as compared with spherocylindrical or semitoroidal aggregates of equal volumes, and their larger aggregate order parameters at equal axial ratios. We must, however, keep in mind that the rotational order parameter S_{DA} in a real system may well have a lower magnitude than in the idealized models. As a consequence of all this, it is not possible to differentiate between the two structural models on the basis of the magnitude of the composite order parameter S_{DM} unless this is very large. The experimental $|S_{DM}|$ values are rather small especially at lower temperatures where the aggregation numbers according to Fletcher [21] are around 90. In our minds this speaks in favour of Fontell's model [19]. The Vargas model [20] can, however, not be completely ruled out since the actual value of S_{AM} is not known. One can easily imagine a structure with oblate aggregates performing a rotation round the cubic directors that is restricted to an extent that gives $S_{DA} \sim 0.6$–0.7. In a 'hard cone' potential of mean torque model [47] this corresponds to a half-cone opening angle of 40°–45°.

In equation (23) the intermediate correlation time τ^s in a crude way gives the time scale for the surfactant reorientation due to lateral diffusion over the aggregate surface and the aggregate rotational diffusion. It is difficult, though, to use the τ^s values to draw quantitative conclusions about the aggregates. To achieve this we present in table 3 results from fittings of the theoretical relaxation rates for Fontell's structure model with spherocylindrical aggregates, equations (6) and (7) with equation (18), to experimental relaxation data. This physical model requires the input of the temperature, the viscosity of water and the length of the surfactant head group which was set to 3.7 Å [21]. The model contains six basic parameters: two for the fast motion, S_{MP} and τ^{MP}, two for the dimensions of the aggregates (we have chosen the small semi-axis of the aggregate R and the volume of the hydrocarbon core V_{hc}), the coefficient of the lateral diffusion of the surfactants over the aggregate surfaces D_{lat}, and the correlation time of the cubic motion τ^{CD}. In addition the coefficient of rotational diffusion perpendicular to the aggregate symmetry axis $R_\perp$ was initially treated as a free parameter. The $R_\perp$ values so obtained varied between 50 and 100% of the hydrodynamic value as given by Yoshizaki and Yamakawa [39] which always was contained within the uncertainties. This variation may seem large, but as can be seen in figure 7, the theoretical relaxation rates are not very sensitive to the $R_\perp$ value in this range. Therefore, $R_\perp$ was fixed to the hydrodynamic value and this had no great influence on the values of the other parameters determined in the fittings. This also implies that a 50% deviation in $R_\perp$ from its hydrodynamic value cannot be detected experimentally. Our results show, however, that the deviation cannot be substantially larger than this. The reason for this is demonstrated in figure 7 where it is shown that theoretical relaxation rates generated with $R_\perp$ set to 0.2 or 0.1 times the hydrodynamic value have characteristic features at intermediate frequencies (1–10 MHz) which originate in the tumbling motions, i.e. the third and fifth terms in equation (11), and which are absent in the experimental data (compare with figures 4 and 5).

In the fittings, we also chose to keep V_{hc} fixed to values calculated from the aggregation numbers obtained by Fletcher [21]. The results obtained for the other five parameters are presented in table 3 where we also give calculated axial ratios ρ and S_{DM} values. It is the

Table 3. Results from fittings of the theoretical relaxation rates for Fontell's structural model, equations (6), (7) and (18), with spherocylindrical aggregates to experimental relaxation data.

T/°C	S_{DM}	τ^{CD}/μs	R^a/Å	ρ^b	D_{lat}/μm^2 s^{-1}	S_{MP}	τ^{MP}/ps	RMS dev./%
25.1	$0.066^{+0.007}_{-0.004}$	$3.5^{+0.7}_{-0.7}$	$20.2^{+0.2}_{-0.3}$	$1.36^{+0.05}_{-0.03}$	73^{+2}_{-2}	$0.205^{+0.002}_{-0.002}$	32^{+2}_{-1}	0.9
41.0	$0.058^{+0.008}_{-0.006}$	$1.7^{+0.5}_{-0.4}$	$20.1^{+0.3}_{-0.3}$	$1.30^{+0.5}_{-0.4}$	108^{+4}_{-4}	$0.198^{+0.003}_{-0.003}$	21^{+1}_{-2}	1.0
55.2	$0.055^{+0.006}_{-0.006}$	$0.75^{+0.21}_{-0.12}$	$19.9^{+0.3}_{-0.3}$	$1.28^{+0.04}_{-0.04}$	150^{+10}_{-20}	$0.188^{+0.007}_{-0.009}$	17^{+3}_{-3}	1.7
60.6	$0.060^{+0.005}_{-0.008}$	$0.38^{+0.04}_{-0.08}$	$19.5^{+0.3}_{-0.3}$	$1.31^{+0.05}_{-0.05}$	160^{+40}_{-20}	$0.181^{+0.020}_{-0.016}$	16^{+4}_{-7}	2.4

[a] The small semi-axis R was not allowed to exceed 20.4 Å [21, 46].
[b] Axial ratio of the aggregates.

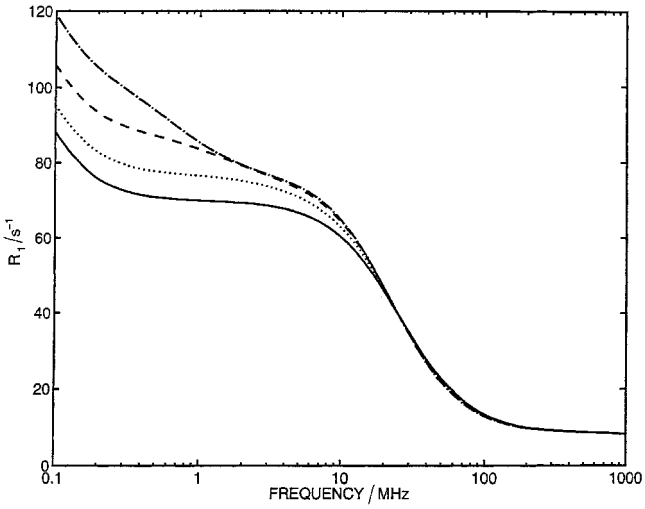

Figure 7. Theoretical ^2H R_1 for Fontell's structural model [19] with spherocylindrical aggregates and the ratio of the effective coefficient of rotational diffusion perpendicular to the aggregate axis to the hydrodynamic value (see the text) set to: 1 (—), 0.5 (···), 0.2 (- - -) and 0.1 (—·—). The other input parameters are the same for all curves, i.e. $T = 41°C$ and $n_a = 82$.

relaxation rates from these fittings that are shown as the solid and dashed lines in figures 4 and 5 where the ability of the model to reproduce the experimental relaxation rates is demonstrated. We see from these figures and the RMS deviations that the quality of the fittings is good, better than that of the three-step fittings. The Vargas model gives equally good fittings, none of which show any systematic deviations from the experimental relaxation rates, which speaks in favour of the general structure and the dynamic model applied. Also, the results obtained here suggest that there is very little change in the phase structure over the temperature interval. The results for S_{DM} obtained by fitting the Fontell model confirm the results of the three-step model. It is also interesting to compare the value $D_{lat} = 73\,\mu m^2\,s^{-1}$ obtained at 25°C from the fittings of the Fontell model to that of $65\,\mu m^2\,s^{-1}$ for a 30% micellar solution at 28°C, which can be estimated form the Lorenztian correlation time for the slow part of the ^2H relaxation dispersion [24] and the aggregation number [22]. The Vargas model with semi-toroidal aggregates, although it fits very well to the data, gives a D_{lat} that is 50% higher than in micelles.

If we look at the correlation time τ^{CD}, it agrees very well with τ^{vs} obtained from the three-step fittings and with τ_{ex} determined from the self-diffusion at the two higher temperatures, but it is ~45% smaller at 25°C. This may partly be an artefact, however. We have until now assumed that our sample acts as a true powder from a relaxation rate point of view. The condition for this is, as pointed out above, that the spatial diffusion over crystallites with different orientations is fast compared with the differences in relaxation rates. With the equations of [29] and the parameters obtained above we can calculate the variation in the relaxation rates with orientation. Calculations of this type show that there is very little variation in R_1; the variation is well within the uncertainties in the experimental values for all temperatures and frequencies. For R_1 our approach is therefore valid. These results also imply that the orientation dependence of R_1 cannot be utilized to extract the spectral densities in a model-free way as is suggested in [29] and this is probably the case for most I_1 phases. The variation in R_2 is, on the other hand, substantial. At 55°C the RMS diffusion length during a time interval corresponding to the maximum difference in R_2 is of the order of μm and it is questionable if the crystallites are small enough for the averaging to be efficient. However, the result from a simulated T_2 experiment, where the intensity for each peak was integrated over the contributions from different orientations with different intensities and linewidths, was equal to the isotropic value within the uncertainties why a failure to meet the above conditions has no consequences for the interpretation of the relaxation rates. At 25°C the diffusion length is a factor of ten smaller and the simulated R_2 15–20% lower than the isotropic R_2. At 41°C the difference is ~5%. At these temperatures, the applied method may therefore well underestimate the isotropic value. Fittings of data sets where the R_2 values were increased with corresponding amounts gave a τ^{CD} at 41°C that agrees quite well with the self-diffusion value while there remains a small difference at 25°C.

5. Discussion

We argue above that the magnitude of the composite rotation–aggregate order parameter S_{DM} cannot be used unambiguously to differentiate between the structural models. The determined S_{DM} values are, however, interesting by themselves. Their constancy over the temperature interval is an important result. It is also interesting to note that they are very close to the value of 0.06 obtained for lysolechitin [26] (determined from the figures in the cited article) and 0.07 for 6-(dimethyleicosylammonio)-hexanoate [22]. These two phases have not been assigned to any space group but their NMR spectra show two kinds of aggregates and this points to the *Pm3n* structure [13]. This suggests that the structure of the *Pm3n* I_1 phase does not change much even in the finer details such as the axial ratios of the aggregates, not only over the large temperature interval but also between the different systems, despite the different characters of the amphiphiles. This, in turn, leads to the suspicion

that the conditions for the formation of this phase may be quite specific and that the aggregate geometry may not vary much.

A study of the published phase diagrams containing I_1 phases and other literature data confirms this view and suggests that it also may apply to I_1 phases other than the *Pm3n* type. In the vast majority of investigated systems, the I_1 phases exist in a concentration interval between 40–50% by weight of aggregates (amphiphiles + additive) in ionic and zwitter-ionic systems, and between 30–40% wt in non-ionic systems. This corresponds to volume fractions of hydrated surfactant [8, 10] that are close to the maximum packing fraction. (For the *Pm3n* structure it is 0.71 for eight spherocylinders and 0.79 for six discs with semi-toroidal rims and two spheres.) It is thus only when the micelles are nearly in contact that it is favourable to form an ordered phase. The loss in entropy associated with the formation of an ordered phase can be overcome by a reduction of the interaggregate repulsion energy, if this is large enough. In ionic systems this repulsion is, of course, mainly of an electrostatic nature which is demonstrated by the substantial effect of the addition of salt on the melting point of the C_{12}TACl I_1 phase [5]. The common occurrence of I_1 phases in systems of non-ionic surfactants shows however that the interaggregate interactions may have other origins. In these systems the repulsive forces are weaker than in ionic systems since the melting points of the I_1 phases are substantially lower [9, 12, 14].

It is further quite clear that another prerequisite for the formation of these phases is that the properties of the amphiphile favour the formation of only slightly anisometric, rather than rod-like, micelles at the concentrations discussed above. This is shown by the fact that the addition of aliphatic hydrocarbons, which are known to cause a rod to globule transition in micellar solutions [48–52], brings about the formation of I_1 phases in many systems where they are not formed by the neat surfactant in water [14, 15]. This point is especially well demonstrated by the results of Oetter and Hoffman [15]. They show that solubilization of larger open chain alkanes which are known to be efficient in shortening rod-like micelles, is also efficient in promoting the formation of I_1 phases in the tetradecyldimethylamine oxide system. For cyclohexane, higher concentrations are required for the formation of a stable I_1 phase in parallel with its observed effect on micellar size and shape [49–52]. If there is any difference between the different types of I_1 phases in this respect cannot be deduced from the literature data.

As mentioned, we found in the fittings that the rate of the tumbling motion does not differ substantially from the hydrodynamical value despite the fact that this motion, for geometrical reasons, has to be strongly concerted, i.e. collective. This could be interpreted as speaking against the structural model in the form in which it has been presented here, but it is easy to imagine a structure with six prolate aggregates and two spherical, the tumbling of which would be governed by hydrodynamics. Such a structure allows a smaller maximum packing fraction than that with eight prolate aggregates, but it should be favoured by the increased entropy in the tumbling motion. The spread in the aggregation numbers determined in a fluorescence quenching study [21] is also sufficient to allow for such a structure [53].

The authors are indebted to Olle Söderman and Bertil Halle for fruitful discussions. This work was financed by the Swedish Natural Sciences Research Council.

References

[1] Fontell, K., 1990, *Colloid Polym. Sci.*, **268,** 264.
[2] Bleasdale, T. A., and Tiddy, G. J. T., 1990, in *The Structure, Dynamics and Equilibrium Properties of Colloidal Systems*, edited by D. M. Bloor, and E. Wyn-Jones (The Netherlands: Kluwer), p 397.
[3] Hoffman, H., 1984, *Ber. Bunsenges. phys. Chem.*, **88,** 1078.
[4] Broome, F. K., Hoerr, C. W., and Harwood, H. J., 1951, *J. Am. chem. Soc.*, **73,** 3350.
[5] Blackmore, E. S., and Tiddy, G. J. T., 1988, *J. chem. Soc. Faraday Trans. 2*, **84,** 1115.
[6] Hagslätt, H., Söderman, O., Jönsson, B., and Johansson L. B.-Å., 1991, *J. phys. Chem.*, **95,** 1703.
[7] Arvidsson, G., Brentel, I., Khan, A., Lindblom, G., and Fontell, K., 1985, *Eur. J. Biochem.*, **152,** 753.
[8] Eriksson, P.-O., Lindblom, G., and Arvidsson, G., 1987, *J. phys. Chem.*, **91,** 846.
[9] Mitchell, D. J., Tiddy, G. J. T., Waring, L., Bostock, T., and McDonald, M. P., 1983, *J. chem. Soc. Faraday Trans. 1*, **79,** 975.
[10] Nilsson, P. G., and Lindman, B., 1983, *J. phys. Chem.*, **87,** 4756.
[11] Nilsson, P.-G., Wennerström, H., and Lindman, B., 1983, *J. phys. Chem.*, **87,** 1377.
[12] Jousma, H., Bouwstra, J. A., Spies, F., and Junginger, H. E., 1987, *Colloid Polym. Sci.*, **265,** 830.
[13] Sakya, P., Seddon, J. M., Templer, R. H., Mirkin, R. J., and Tiddy, G. J. T., 1997, *Langmuir*, **13,** 3706.
[14] Ekwall, P., 1975, *Adv. Liq. Cryst.*, **1,** 1.
[15] Oetter, G., and Hoffman, H., 1989, *Colloids Surf.*, **38,** 225.
[16] Balmbra, R. R., Clunie, J. S., and Goodman, J. F., 1969, *Nature*, **222,** 1159.
[17] Tardieu, A., and Luzzati, V., 1970, *Biochem. Biophys. Acta*, **219,** 11.
[18] Bull, T., and Lindman, B., 1974, *Mol. Cryst. liq. Cryst.*, **82,** 155.
[19] Fontell, K., Fox, K. K., and Hansson, E., 1985, *Mol. Cryst. liq. Cryst. Lett.*, **1,** 9.
[20] Vargas, R., Mariani, P., Gulik, A., and Luzzati, V., 1992, *J. mol. Biol.*, **225,** 137.

[21] Fletcher, P. D. I., 1988, *Mol. Cryst. liq. Cryst.*, **154,** 323.
[22] Johansson, L. B.-Å., and Söderman, O., 1987, *J. phys. Chem.*, **91,** 5275.
[23] Söderman, O., and Johansson, L. B.-Å., 1996, *J. colloid interface Sci.*, **179,** 570.
[24] Söderman, O., Walderhaug, H., Henriksson, U., and Stilbs, P., 1985, *J. phys. Chem.*, **89,** 3693.
[25] Söderman, O., and Henriksson, U., 1987, *J. chem. Soc. Faraday Trans. 1*, **83,** 1515.
[26] Eriksson, P.-O., Lindblom, G., and Arvidsson, G., 1985, *J. phys. Chem.*, **89,** 1050.
[27] Quist, P.-O., Halle, B., and Furò, I., 1992, *J. chem. Phys.*, **96,** 3875.
[28] Sitnikov, R., Furò, I., Tòth, F., and Henriksson, U., *Rev. sci. Instr.* (in the press).
[29] Halle, B., 1992, *Liq. Cryst.*, **12,** 625.
[30] Gustafsson, S., and Halle, B., 1993, *Mol. Phys.*, **80,** 549.
[31] Halle, B., and *Wennerström, H.*, 1981, *J. chem. Phys.*, **75,** 1928.
[32] Halle, B., 1991, *J. chem. Phys.*, **94,** 3150.
[33] Törnblom, M., Henriksson, U., and Ginley, M., 1994, *J. phys. Chem.*, **98,** 7041; Erratum 1997, *J. phys. Chem.*, **101,** 3901.
[34] Brink, D. M., and Satchler, G. R., 1993, *Angular Momentum* (Oxford: Clarendon Press).
[35] Perrin, F., 1934, *J. Phys. Radium*, **5,** 497.
[36] Woessner, D. E., 1962, *J. chem. Phys.*, **37,** 647.
[37] Abragam, A., 1961, *The Principles of Nuclear Magnetism* (Oxford: Clarendon Press), Chap. 8.
[38] Halle, B., personal communication.
[39] Yoshizaki, T., and Yamakawa, H., 1980, *J. chem. Phys.*, **72,** 57.
[40] Montgomery, J. A., and Berne, B. J., 1977, *J. chem. Phys.*, **67,** 4598.
[41] Nery, H., Söderman, O., Canet, D., Walderhaug, H., and Lindman, B., 1986, *J. phys. Chem.*, **90,** 5802.
[42] Walderhaug, H., Söderman, O., and Stilbs, P., 1984, *J. phys. Chem.*, **88,** 1655.
[43] Jansson, M., Li, P., Henriksson, U., and Stilbs, P., 1989, *J. phys. Chem.*, **93,** 1448.
[44] Söderman, O., 1986, *J. magn. Reson.*, **68,** 296.
[45] Furò, I., and Halle, B., 1995, *Phys. Rev. E*, **51,** 466.
[46] Tanford, C., 1980, *The Hydrophobic Effect* (New York: John Wiley).
[47] Wang, C. C., and Pecora, R., 1980, *J. chem. Phys.*, **72,** 5333.
[48] Lindemuth, P. M., and Bertrand, G. L., 1993, *J. phys. Chem.*, **97,** 7769.
[49] Hoffman, H., and Ulbricht, W., 1987, *Tenside Surfactants Detergents*, **24,** 23.
[50] Bayer, O., Hoffman, H., Ulbricht, W., and Thurn, H., 1986, *Adv. colloid surf. Sci.*, **26,** 177.
[51] Hoffman, H., and Ulbricht, W., 1989, *J. colloid interface Sci.*, **129,** 388.
[52] Törnblom, M., and Henriksson, U., 1997, *J. phys. Chem. B*, **101,** 6028.
[53] Söderman, O., personal communication.